

Water-sensitive Gelatin Phantoms for Skin Water Content Imaging

Gennadi Saiko¹ ^a and Alexandre Douplik² ^b

¹Swift Medical Inc, 1 Richmond St. W., Toronto, Canada

²Department of Physics, Ryerson University, Toronto, Canada

Keywords: Multispectral Imaging, Tissue Phantoms, Skin Water Content, Skin Moisture.

Abstract: Oxygen supply to tissues can be seriously impacted during wound healing. Edema (accumulation of fluids in interstitial space) can increase the distance between capillaries, thus decreasing oxygen supply to cells. There is no standard clinical tool for quantification of edema, and early edema detection (preferably preclinical) is of great clinical need. Multispectral imaging can be a helpful clinical tool to characterize water content in the skin. However, to develop and validate this technology, a reliable water-sensitive preclinical model has to be developed. The scope of this work is to develop a water-responsive skin model and assess the feasibility of extracting water content using multispectral imaging. **Methods:** A phantom fabrication protocol has been developed. The phantoms are based on the gelatin crosslinked with glutaraldehyde. TiO₂ nanoparticles were added to mimic the optical properties of the skin. To emulate various water content, phantoms were dipped in the water for various duration. The phantoms were imaged using the Multi-Spectral Imaging Device (MSID) (Swift Medical Inc, Toronto). MSID is a multispectral imaging system for visualization of tissue chromophores in surface tissues. It uses 12-bit scientific-grade NIR-enhanced monochrome camera (Basler, Germany) and ten wavelength light source (600-1000nm range) to visualize the distribution of oxy-, deoxyhemoglobins, methemoglobin, water, and melanin. The imaging distance is 30cm, the field of view: 7x7cm. **Results:** Initial results show that the developed model mimics the optical scattering properties of the skin. MSID was able to extract water content using a full set (ten wavelengths) and a subset (three wavelengths) of channels. **Conclusions:** A new water responsive model for skin moisture imaging has been developed. Initial experiments with multispectral imaging of these phantoms show feasibility of tissue water content imaging with Si-based cameras.


1 INTRODUCTION


Edema (accumulation of fluids in interstitial space) is a common clinical sign in a wide variety of conditions. Being a nonspecific finding it often poses a challenge for the clinician. While in many cases, it has a benign origin, in other instances, it can be a sign of life-threatening conditions. Because the interstitium can easily accommodate several liters of fluid, a patient's weight may increase by nearly 10% before pitting edema is evident. Thus, early detection of edema (preferably preclinical) is of great importance, especially for patients with compromised health (diabetes, kidney or heart conditions, etc.).

Edema can seriously impact wound healing by restricting oxygen supply to tissues. For example,

edema can increase the distance between capillaries, thus decreasing oxygen supply to cells, or it may compress small vessels to shut off the local blood supply at all, thus creating necrotic tissue.

There is no standard for an objective measurement of edema. In particular, for peripheral edema, the most widely-used technique is a subjective clinical assessment where an examiner applies pressure with an index finger to the patient's ankle (Seidel, 1995) to capture pit depth and the time needed for the skin to return to its original state (recovery time). Despite common use, this method has not been proven to be a sufficiently objective, reliable, or sensitive assessment of edema. Several quantitative methods to measure peripheral edema have been proposed, but they are mostly used in physical therapy and sports medicine: patient questionnaire, ankle circumference

^a  <https://orcid.org/0000-0002-5697-7609>

^b  <https://orcid.org/0000-0001-9948-9472>

(Mora, 2002), figure-of-eight (Mawdsley, 2000), edema tester (Cesarone, 1999), indirect leg volume (by series of ankle/leg circumferences) (Latchford, 1997), and water-displacement volumetry (Kaulsar Sukul, 1993).

Several quantitative technologies have been used to assess edema or the hydration of skin non-invasively. They include skin impedance methods, ultrasound, and magnetic resonance imaging, and spectroscopy.

The major part of existing methods of measuring of edema suffers from various shortcomings; namely, subjectivity (Brodovicz, 2009), inability to detect on early stages (Hedlund, 1985), and impossibility to be applied in certain clinical or field settings (e.g., water displacement for postoperative patients, MRI, and ultrasound in field settings).

Thus, it would be useful to have a more widely accessible way to investigate edema and ideally visualize it in various clinical and field settings.

Optical spectroscopy and imaging, along with the skin impedance measurements (Mayrovitz, 2007), are promising modalities for the non-invasive diagnosis and monitoring of skin water content. However, optical imaging has several inherited advantages over skin impedance measurements: a) it is able to visualize (image) the large field of view, while skin impedance techniques are essentially one point measurements, prone to operator's errors, b) it is a remote measurement, while skin impedance requires contact with the skin and sterilization after each use.

Thus, optical water content imaging would be a useful clinical tool adjuvant to diagnostics of peripheral vascular disease and pressure injuries.

However, the development of such imaging technology is complicated in part due to the lack of the gold standard and established water responsive models. For example, its comparison and/or validation with skin impedance techniques is not a straightforward task such as various geometries of skin impedance probes have different sampling depths, which can be incomparable with an optical sampling depth at a particular wavelength.

Thus, one of the important steps in developing the water content imaging modality is to develop a controllable water-responsive model, which can be used to validate/calibrate the technology in the absence of the gold standard.

While multiple experimental (Pogue, 2006; Ohmae, 2018) and computational (Kainz, 2018) models have been developed to mimic the optical and RF properties of the human tissues, still there is a need in versatile water-responsive models.

Our group works on multispectral imaging moda-

lities adjuvant to tissue oximetry. In our previous works, we have developed several phantom models and demonstrated the feasibility of multispectral visualization of methemoglobin in the tissue (Saiko, 2018).

This scope of this work is to develop a water-responsive skin model and assess the feasibility of multispectral imaging of water content in the skin.

2 METHODS

Water content within the stratum corneum gradually increases from about 10% to about 30% between the surface and deeper layers, followed by an abrupt increase to about 70% in the epidermis (Warner, 1988).

The water content of the different skin layers is of interest in different fields. While the water content of the epidermis is the primary interest in the skincare industry, subepidermal water accumulation is of interest in wound care.

Water content imaging of the different skin layers can be based on various light absorption bands. Water absorption at 1440nm is 30 times stronger than at 1190nm, which in turn more than two times stronger than absorption at 970nm. Given this hierarchy and corresponding light penetration depths it is possible to expect that 1440nm and 1920nm wavelengths are suitable for imaging of water content in uppermost skin layers (stratum corneum), while 970nm and 1190nm can be used for water content determination and imaging in deeper skin layers, including epidermis, dermis (1190nm) and even subcutaneous tissues (970nm). Illumination of the skin with these wavelengths will integrate signals from various depths (up to a few millimeters) and thus will not be sensitive to skin conditions in surface layers, which due to their small thickness and low water content account only for a small fraction of water in integration volume.

For our purposes, we selected 970nm range, which a) have the required sampling depth (dermis and subcutaneous tissues), and b) can be implemented using inexpensive Si-based sensors.

To explore the feasibility of quantification of water content in the skin, we have developed a water-responsive skin model. The model is based on a mechanical gelatin-based human skin model (Dabrowska, 2017) with adaptations to mimic the optical parameters of the skin.

2.1 Materials

The phantoms were based on the type A gelatine derived from porcine skin, with 300 g gel strength (G2500, Sigma-Aldrich, Canada), which does not have significant optical absorption and scattering in the visible range. Each phantom contained 10% (w/w) of type A gelatin.

TiO₂ particles (Sigma-Aldrich, Canada) were used to mimic the scattering property of the skin.

Glutaraldehyde (Sigma Aldrich, Canada) was used for the cross-linking of gelatin.

2.2 Phantom Fabrication

We have developed the following protocol for phantom fabrication:

1. Prepare a 10 wt% solution of gelatine (type A, bloom no 300, Sigma Aldrich) in distilled water by continuous stirring at 60 °C for 2 h.
2. Mix with a known concentration of a scattering agent (TiO₂ nanoparticles).
3. Place the final solution in an ultrasonic bath at a temperature of 37 – 38 degrees to degas for 2 minutes to disrupt the air bubbles trapped inside the phantom,
4. Pour the solution into the Petri dish (with wax paper layer) to solidify: 2mm layer.
5. Leave the phantom to dry for 24 h at room temperature.
6. Gelatin crosslinking: Place the phantom in 1 wt% solution of glutaraldehyde (Sigma Aldrich) in Dulbecco's PBS buffer (DPBS, GIBCO) for 24 h at room temperature under continuous stirring (130 rpm).
7. Rinse phantoms with distilled water.
8. Dry phantoms by wrapping in paper towels and placing between two boards with the use of weight, to avoid ripples caused by drying-related contraction.
9. Change paper towels daily and measure the weight of each phantom. It is considered to be dry after mass stabilization (about 6 days).

To emulate various hydration levels in the skin, the samples were dipped in the water for various time. Electronic scales measured weight before and after dipping.

2.3 Imaging

The Multi-Spectral Imaging Device (MSID) (Swift Medical Inc, Toronto) is a multispectral imaging system (see Figure 1) for visualization of the distribution of oxy-, deoxyhemoglobins,

methemoglobin, water, and melanin in the skin. The MSID consists of a 10-channel illumination unit, a scientific-grade camera (a 12-bit NIR-enhanced monochrome camera acA1300-60gmNIR (Basler, Germany)), and a processing unit, which coordinates them and collect data. Ten channels of the illumination unit illuminate the target area with 630, 660, 690, 735, 810, 830, 850, 880, 940, and 970nm, respectively. Each channel consists of 4 high power LEDs arranged into a circle. The illumination unit produces a sequence of light flashes, each flash at a particular wavelength, while the camera captures a series of images, each with illumination at particular wavelength. The acquired images are arranged into a 3D hypercube (λ, i, j) for further processing. The imaging distance is 30cm, the field of view: 7x7cm.

2.4 Image Processing

During each measurement, the MSID device captures 11 images: ten with illumination at a particular wavelength and one without additional illumination (ambient light only). The processing consists of the following consequential steps: a) calculate diff images (subtract the image without additional illumination from the image with illumination at a particular wavelength), b) obtain reflectance images by dividing the diff image on the diff image of the reference object, c) extract index of absorption μ_a from reflectance using tissue light transport model (e.g., Beer-Lambert), d) extract tissue chromophore concentrations using least square fitting.

To emulate a compact device scenario, various subsets of captured images (10 or 3 of them) were used to extract water content.

The MSID device uses the 12bit scientific-grade camera (acA1300-60gmNIR (Basler, Germany)).

False-color maps were used to visualize water content.

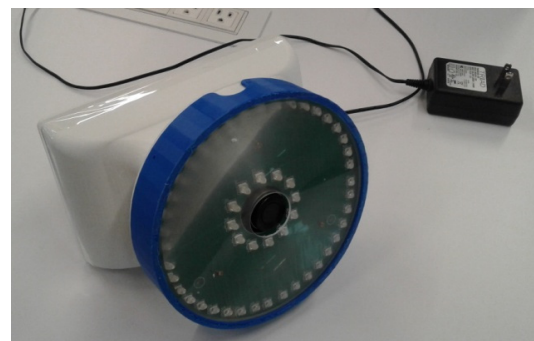


Figure 1: Multi-Spectral Imaging Device (MSID).

3 RESULTS

Rough calculations based on the model developed in (Saiko, 2019) show that we can expect approximately -0.4% change in reflectance for every 1% increase in the absorption coefficient at 970nm. Given that the water is the primary absorber in this range we can expect that it will be possible to detect even preclinical peripheral edema with an expected increase in water content. In particular, we expect that a 50% increase in interstitial fluid volume for water content in the skin, adipose tissue, connective tissue will translate into a 5-6% increase in total tissue water content (see Table 1). This increase will translate into -2.0...-2.4% change in tissue reflectance, which is possible to detect even using an 8-bit camera.

The developed phantoms were visualized using MSID. To emulate various water content in the tissue, phantoms were dipped in the water for the various duration.

Table 1: Initial and expected water content for different tissue types.

| Tissue | Initial water content, % (Braunwald, 1994) | Expected water content for 50% increase in IFV, % |
|-------------------|--|---|
| Skin | 72 | 79 |
| Skeletal muscle | 76 | 77.4 |
| Adipose tissue | 14 | 18.5 |
| Connective tissue | 80 | 86 |

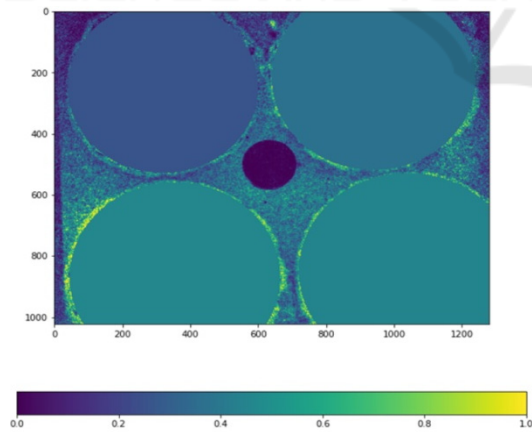


Figure 2: Water content extraction using ten wavelengths. Dry sample (upper left), sample dipped for several seconds (top right), 5 min (bottom left), and 20 min (bottom right).

The results of water content extraction using all ten channels and three channels are presented in Figure 2 and Figure 3, respectively. Four samples on these figures have various water content: dry sample (upper left), and samples dipped for several seconds

(top right), 5 min (bottom left) and 20 min (bottom right).

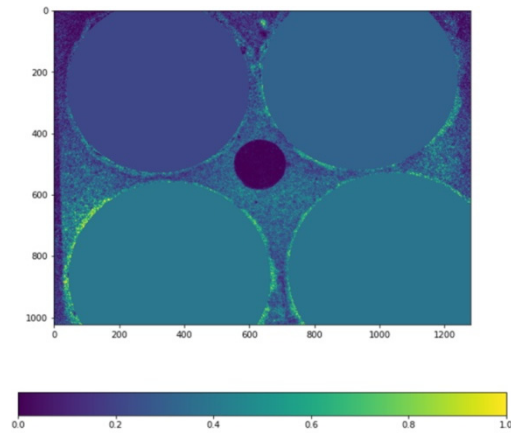


Figure 3: Water content extraction using three wavelengths. Dry sample (upper left), sample dipped for several seconds (top right), 5 min (bottom left), and 20 min (bottom right).

4 DISCUSSION

Our initial calculations show that the multispectral/hyperspectral imaging using a 970nm band and Si-based sensor can retrieve clinically relevant changes in the tissue water content.

These calculations were supported by our initial experiments on phantoms, which demonstrate the feasibility of water content imaging using Si-based cameras. The water content was successfully extracted using the full set of channels (10 channels) and its subset (3 channels, including 970nm). Results are almost identical, so we can conclude that three illumination wavelengths may be sufficient for water content visualization. These results are in line with preliminary experiments on volunteers reported separately (Saiko, 2020).

Initial experiments also show that the developed gelatine-based phantoms a) demonstrate optical properties similar to the skin, and b) demonstrate required water-responsive properties. We will report phantom validation results separately. The current study with dipping phantoms in the water was a proof-of-concept. In the future, we plan to vary phantom water content in a more quantifiable way by spreading a certain amount of water over its surface and comparing water content results with those obtained by bioimpedance measurements.

It should be noted that the cross-linked phantoms changed their color from clear to pink during crosslinking. In future work, we plan to investigate

these color changes and find conditions that minimize them or investigate other cross-linking agents.

5 CONCLUSIONS

A new water responsive model for skin water content imaging has been developed. Initial experiments with multispectral imaging of these phantoms show the feasibility of tissue water content imaging with Si-based cameras using a 970nm band.

ACKNOWLEDGEMENTS

Authors are thankful to Burhan Hussein and Andrei Betlen for help with phantom fabrication and image processing.

REFERENCES

- Seidel H.M, Ball J.W, Dains J.E, et al., 1995. *Heart and blood vessels*. In: Schrefler S, ed. *Mosby's Guide to Physical Examination*, St. Louis, MO: Mosby. 3rd ed.
- Mora S, Zalavras C.G, Wang L, Thordarson DB, 2002. The role of pulsatile cold compression in edema resolution following ankle fractures: a randomized clinical trial. *Foot Ankle Int*, 23:999-1002.
- Mawdsley R.H, Hoy D.K, Erwin P.M, 2000. Criterion-related validity of the figure-of-eight method of measuring ankle edema. *J Orthop Sports Phys Ther*, 30:149-153.
- Cesarone M.R, Belcaro G, Nicolaides A.N, Arkans E, Laurora G, De Sanctis MT, Incandela L, 1999. The edema tester in the evaluation of swollen limbs in venous and lymphatic disease. *Panminerva Med*;41:10-14.
- Latchford S, Casley-Smith J.R, 1997. Estimating limb volumes and alterations in peripheral edema from circumferences measured at different intervals. *Lymphology*; 30:161-164.
- Kaulesar Sukul D.M, den Hoed P.T, Johannes E.J, van Dolder R, Benda E., 1993. Direct and indirect methods for the quantification of leg volume: comparison between water displacement volumetry, the disk model method and the frustum sign model method, using the correlation coefficient and the limits of agreement. *J Biomed Eng*; 15:477-480.
- Brodovicz K.G, McNaughton K, Uemura N, Meininger G, Girman CJ, Yale SH., 2009. Reliability and Feasibility of Methods to Quantitatively Assess Peripheral Edema. *Clin Med & Res* ; 7(1-2):21-31.
- Hedlund LW, Putman C.E, 1985. Methods for detecting pulmonary edema, *Toxicol Ind Health*. 1(2):59-68.
- Mayrovitz H.N, 2007. Assessing local tissue edema in postmastectomy lymphedema, *Lymphology* 40: 87-94.
- Pogue B.W. and Patterson M. S, 2006. Review of tissue simulating phantom for optical spectroscopy, imaging and dosimetry, *JBO*. 11(4), 041102.
- Ohmae E., Yoshizawa N., Yoshimoto K., Hayashi M., Wada H., Mimura T., Suzuki H., Homma S., Suzuki N., Ogura H., Nasu H., Sakahara H., Yamashita Y., and Ueda Y., 2018. Stable tissue-simulating phantoms with various water and lipid contents for diffuse optical spectroscopy, *BOE* 9, 5792-5808.
- Kainz, W., Neufeld E., Bolch W., Graff C., Kim C. H., Kuster N., Lloyd B., Morrison T., Segars P., Yeom Y., Zankl M., Xu G., Tsui B., 2018, Advances in Computational Human Phantoms and Their Applications in Biomedical Engineering -A Topical Review. *IEEE Trans Rad and Plasma Med Scie.*, 3(1): 1-23.
- Saiko G, Zheng X, Betlen A, Douplik A, 2018. Visualization of Methemoglobin Distribution in Tissues: Phantom Validation, *Adv Exp Med Biol* 1072, 387-390
- Braunwald E., 1994. Edema. In. *Harrison's Principles of Internal Medicine*, Isselbacher KJ, Braunwald E, Wilson JD, et al., eds. New York: McGraw-Hill; 13th ed.
- Bhave G, Neilson E.G , 2011, Body Fluid Dynamics: Back to the Future, *JASN*, 22(12): 2166-2181.
- Saiko G, Betlen A, 2019, Optimization of Band Selection in Multispectral and Narrow-Band Imaging: an Analytical Approach, *Adv Exp Med Biol*. (in press)
- Dąbrowska A., Rotaru G.M., Spano F., Affolter Ch., Fortunato G., Lehmann S., Derler S., Spencer N.D., Rossi R.M., 2017. A water-responsive, gelatine-based human skin model, *Tribology Int*, 113, 316-322.
- Warner R., Myers M. C., and Taylor D. A., 1988. Electron probe analysis of human skin: Determination of the water concentration profile, *J. Invest. Dermatol.* 90, 218-224.
- Saiko G., 2020. On the feasibility of skin water content imaging adjuvant to tissue oximetry, *Adv Exp Med Biol* (accepted).